Lujan Facundo, MJ.; Fernández-Navarro, J.; Alonso Molina, JL.; Amoros, I.; Moreno Trigos, MY.; Mendoza Roca, JA.; Pastor Alcañiz, L. (2018). The role of salinity on the changes of the biomass characteristics and
on the performance of an OMBR treating tannery wastewater. Water Research. 142:129-137. https://doi.org/10.1016/j.watres.2018.05.046

The role of salinity on the changes of the biomass characteristics and on the performance of an OMBR treating tannery wastewater

M.J. Luján-Facundo[1], J. Fernández-Navarro[2], J.L. Alonso-Molina[2], I. Amorós-Muñoz[2], Y. Moreno[2], J.A. Mendoza-Roca[1], L. Pastor-Alcañiz[3].

[1]Instituto de Seguridad Industrial, Radiofísica y Medioambiental, Universitat Politècnica de València, Camino de Vera, s/n, Valencia 46022 (Spain).

[2]Instituto de Ingeniería del Agua y Medio Ambiente, Universitat Politècnica de València, Camino de Vera, s/n, Valencia 46022 (Spain).

[3]Depuración de Aguas del Mediterráneo (DAM). Avenida Benjamín Franklin, 21. 46980 Parque Tecnológico, Paterna, Valencia (Spain).

Tel. +34963876386

e-mail: malufa@etsii.upv.es

Keywords: Forward osmosis, Osmotic membrane bioreactor, Tannery wastewater, Draw solution, microbial community.

Abstract

Tannery wastewaters are difficult to treat biologically due to the high salinity and organic matter concentration. Conventional treatments, like sequential batch reactors (SBR) and membrane bioreactors (MBR), have showed settling problems, in the case of

SBR, and ultrafiltration (UF) membrane fouling in the case of MBR, slowing their industrial application. In this work, the treatment of tannery wastewater with an osmotic membrane bioreactor (OMBR) is assessed. Forward osmosis (FO) membranes are characterized by a much lower fouling degree than UF membranes. The permeate passes through the membrane pores (practically only water by the high membrane rejection) from the feed solution to the draw solution, which is also an industrial wastewater (ammonia absorption effluent) in this work. Experiments were carried out at laboratory scale with a FO CTA-NW membrane from Hydration Technology Innovations (HTI). Tannery wastewater was treated by means of an OMBR using as DS an actual industrial wastewater mainly consisting of ammonium sulphate. The monitoring of the biological process was carried out with biological indicators like microbial hydrolytic enzymatic activities, dissolved and total adenosine triphosphate (ATP) in the mixed liquor and microbial population. Results indicated a limiting conductivity in the reactor of 35 $mS \cdot cm^{-1}$ (on the 43th operation day), from which process was deteriorated. This process performance diminution was associated by a high decrease of the dehydrogenase activity and a sudden increase of the protease and lipase activities. The increase of the bacterial stress index also described appropriately the process performance. Regarding the relative abundance of bacterial phylotypes, 37 phyla were identified in the biomass. Proteobacteria were the most abundant (varying the relative abundance between 50.29% and 34.78%) during the first 34 days of operation. From this day on, Bacteroidetes were detected in a greater extent varying the relative abundance of this phylum between 27.20% and 40.45%.

1. Introduction

Tannery industry belongs to the most polluting industrial sectors (Kandasamy et al., 2017; Maharaja et al., 2017). This industry generates huge volumes of potentially toxic wastewaters characterized by high organic matter and salt concentration. In order to transform raw skins into finished leather products, three groups of processes have to be carried out: beamhouse operations (for flesh, hair and epidermis removal from the skin), tanning steps (to stabilize and avoid putrefaction) and final processes, in which the leathers are finished, acquiring the desired aesthetic appeal and commercial value (Mosca et al., 2017). Typically, beamhouse operations generate alkaline effluents and tanning steps and final processes generate acidic effluents (Drioli et al., 1980; Mendoza-Roca et al., 2010).

The most common treatment of the global effluents is based on a sulfide oxidation of the alkaline stream, a subsequent homogenization of desulfurized alkaline wastewater and acidic streams and a physic-chemical process of the global wastewater. The aim of the physic-chemical treatment is to reduce suspended solids and chemical oxygen demand (COD) content and to remove chromium by precipitation (George et al., 2015; Galiana-Aleixandre et al., 2007). However, the remaining high COD and salt concentrations require further treatments to meet the discharge limits. In this way, it is necessary to apply biological treatments to reduce the organic matter content. Membrane bioreactors (MBR) produce effluents with higher quality than conventional biological treatments (Wang et al., 2016) and are also employed for industrial wastewaters (Le-Clech et al., 2006; Yang et al., 2006). MBR are characterized by high sludge retention time and low reactor volume. However, the main limitations of their

application are the high energy consumption and the high maintenance costs due to the frequent membrane cleaning (Suganthi et al., 2013).

Recent research advances in wastewater treatment and reuse have promoted the development, as an emerging technology, of OMBR (Luo et al., 2016). OMBR uses FO membranes to separate treated water from a bioreactor mixed liquor. The separation process is produced because of the osmotic pressure difference between the biological reactor and the draw solution (DS) (Luján-Facundo et al., 2017; Wang et al., 2016). The use of the FO nonporous membranes offers important advances such as high rejection capacity for trace organic compounds (Xie et al., 2012), pathogens (Hoover et al., 2011) and ions (Hickenbottom et al., 2013), low membrane fouling and the energy consumption. However, the reverse salt flux (RSF) due to the Fick's law and the accumulation of non-biodegradable substances in the reactor originate operating problems in the OMBR. Salinity build-up in the biological reactor may significantly reduce the membrane water flux, modifying the mixed liquor characteristics and enhancing scaling phenomena (Gu et al., 2015). Thus, the impact of solutes accumulation on sludge properties and on microbial community and its activity is one of the most important issues to be studied in OMBR. In this way, parameters such as microbial hydrolytic enzymatic activities (MHEA), intracellular and extracellular ATP, cellular viability and the study of the microbial population will give valuable information about the OMBR process (Nguyen and Chong, 2015).

The changes in the biomass characteristics during the OMBR operation have been evaluated by a limited number of authors. Wang et al. (Wang et al., 2017b) studied the bacterial community analysis for the removal of silver nanoparticles from simulated wastewater using a combination of microfiltration with OMBR. They found that the main phylum in the sludge was *Proteobacteria* and the relative abundance of this

phylum decreased as salt concentration increased. Luo et al. (Luo et al., 2017) compared the microbial community structure of a conventional MBR with that found in an OMBR. They concluded that there were differences between each community analysis such as the presence of *Planctomycetes* only in the MBR and the increase in the relative abundance of *Bacteroidetes* during the OMBR operation time. Qiu and Ting, 2013 studied the effect of salt accumulation on microbial community during a OMBR operation. They published that almost all the dominant species in the sludge were replaced by salt-tolerant new species as a consequence of salinity build-up.

The main objective of this paper is to study how the characteristics of the biomass change with the operation time of an OMBR treating tannery wastewater using an actual industrial wastewater mainly consisting of ammonium sulphate as DS. Until now, the study of the performance of an OMBR process focusing on the biomass characteristics using two actual effluents (as feed and as draw solutions) cannot be found in the literature. In this work, the OMBR mixed liquor proposed characterization includes MHEA, ATP, bacterial viability and microbial population. The relation of these mixed liquor characteristics and accumulated COD and salts in the OMBR during its operation is assessed.

2. Materials and methods

2.1. Wastewater and draw solution

An actual wastewater from a tannery industry was used as influent. The main characteristics of this wastewater were: COD between 1,497 and 3,468 $mg \cdot L^{-1}$, pH in the range of 8.04-9.29 and conductivity varying from 10.8 to 19.41 $mS \cdot cm^{-1}$. An actual wastewater from an absorption process for ammonia removal was employed as DS. This wastewater mainly consisted of ammonium sulphate (SO_4^{-2} and NH_4-N concentrations of 153 $g \cdot L^{-1}$ and 19 $g \cdot L^{-1}$, respectively). The pH and conductivity of this industrial wastewater were 1.2 and 130 $mS \cdot cm^{-1}$, respectively. In this way, pH had to be adjusted to 4.0 in order not to damage the FO membrane.

2.2. OMBR plant and operating conditions

The laboratory OMBR plant used in this experiment was described in a previous study (Luján-Facundo et al., 2017). In order to evaluate the FO membrane water flux and the RSF, the water mass permeated from the biological reactor to the draw solution was registered each 20 minutes using a digital balance PKP (Kern Instruments, Germany) and the software “Kern Balance Connection SCD-4.0”. In addition, the draw and feed solutions conductivities were also registered each 20 minutes by means of two conductivity meters model CDH-DS1 from Omega Engineering (United Kingdom). The used FO commercial membrane was CTA-NW from Hydration Technology Innovations (HTI, USA) made with cellulose triacetate and supported by an embedded polyester screen. In previous studies (Luján-Facundo et al. 2017), results regarding the

145 characterization of this membrane have been described. Thus, membrane water fluxes
146 between 1.6 and 7.8 LMH and reverse salt fluxes between 1.4 and 2.8 $g \cdot m^{-2} \cdot h^{-1}$ were
147 reported for NaCl concentrations in DS between 25 and 200 $g \cdot L^{-1}$.
148
149 Membrane water flux and COD removal efficiency were measured to study the OMBR
150 performance. The membrane water flux (J_w, LMH) was calculated following the Eq. 1:
151

$$J_w = \frac{\Delta V}{A \cdot \Delta t} \quad (1)$$

152 Where, ΔV represents the total volume increase in the DS tank (L) in a time period Δt
153 (h) and A is the active FO membrane area (m^2).

154 Finally, COD removal efficiency was calculated three times per week measuring the
155 COD in the soluble fraction of the biological reactor.
156
157 The sludge used to inoculate the biological reactor was taken from the secondary
158 treatment of a municipal wastewater treatment plant (located in Valencia, Spain). The
159 tannery wastewater was mixed with synthetic wastewater (solution made with
160 bacteriological peptone and meat extract, Panreac, Spain) increasing the amount of
161 tannery wastewater in the reactor feed progressively. It was decided to mix again
162 tannery and synthetic wastewater after 40 days of operation due to the high conductivity
163 in the reactor. The simulated wastewater was always prepared with the same COD as
164 the tannery wastewater. In addition, tri-sodium phosphate 12-hydrate (Panreac, Spain)
165 was added to achieve a COD:N:P relation of 100:5:1.
166

The initial mixed liquor suspended solids (MLSS) concentration in the OMBR was 5 $g \cdot L^{-1}$. During the whole operation, the hydraulic retention time (HRT) varied in the range of 2.86-13.78 days, depending on the membrane water flux. The reactor was fed once a day providing the same wastewater volume as the drawn water volume in order to maintain constant the reaction volume. The food to microorganism (F/M) ratio was determined for the different tannery wastewater samples treated and it ranged between 0.11 and 0.33 g $COD \cdot g\ SS^{-1} \cdot d^{-1}$. The reactor was operated including an anoxic phase after the wastewater supply.

Regarding membrane cleaning protocol, FO membrane was cleaned twice a week according to the details given in a previous work (Luján-Facundo et al., 2017).

2.3. DNA analysis

DNA was measured using Quant-it™ dsDNA HS (0.2–100 ng) kit (Molecular probes, Eugene, OR, USA). The procedure consisted of mixing 10 µL of standard or sample with 190 µL of Quant-it working solution. Each sample was stored at room temperature for 2 min. Finally, DNA concentrations were measured in the Qubit fluorometer.

2.4. MHEA

Table 1 shows the seven MHEA that were measured together with the substrate, reaction product and the wavelength at which absorbance was measured. 1.0 mmol of reaction product produced in 1 hour was used to establish the definition of the corresponding enzyme unit (EU).

Before MHEA analysis the mixed liquor samples were centrifuged at 2500 rpm for 2 min and wastewater was drained to eliminate substances that could produce interference in the analysis. The pellet of activated sludge was re-suspended in the same amount of Tris-HCl buffer (0.2 $mol \cdot L^{-1}$, pH 7.6) to preserve the VSS concentration. The absorbances were measured with a Thermo Scientific™ 9423UVG1002E spectrophotometer. More details about the MHEA measurement can be found in Ferrer-Polonio et al. (Ferrer-Polonio et al., 2017). The EU values were divided by the MLVSS ($g \cdot L^{-1}$).

Table 1: MHEA analyzed during the OMBR operation.

MHEA	Substrate	Reaction product	Wavelength (nm)
Alkaline phosphatase	4-Nitrophenyl phosphate bis(tris) salt	p-Nitrophenol	410
Acid phosphatase	4-Nitrophenyl phosphate bis(tris) salt	p-Nitrophenol	410
Dehydrogenase	Iodonitrotetrazolium chloride	1,3,5-Triphenyltetrazolium formazan	490
Lipase	4-Nitrophenyl palmitate	p-Nitrophenol	410
Protease	Azocasein	Colored Unknown peptides	340
α-D-Glucosidase	4-Nitrophenyl α-D-glucopyranoside	p-Nitrophenol	410
β-D-Glucuronidase	4-Nitrophenyl β-D-glucuronide	p-Nitrophenol	410

206 2.5. ATP

207 ATP was measured by QG21Waste™ kit using PhotonMaster™ Luminometer from
208 Luminultra®. The equipment calibration was carried out by a standard solution of
209 Luminase and volumes of 1.0 mL and 100 µL of activated sludge were used to quantify
210 total-ATP (tATP) and dissolved-ATP (dATP). The tATP is the sum of intracellular and
211 extracellular ATP and the dATP is the ATP present outside living cells and rejected by
212 dead microorganisms. The results were determined in RLU (Related Luminescence
213 Units) and were converted to ng ATP·mL^{-1} using a Standard ATP solution
214 UltraCheck™. Biomass Stress Index (BSI), which represents the microorganisms stress
215 or mortality, and Active Volatile Suspended Solids (AVSS) were calculated from the
216 ATP data.
217

218 2.6. Bacterial community analysis

219 Five activated sludge samples named S1 (day 6), S2 (day 20), S3 (day 34), S4 (day 48)
220 and S5 (day 55) were collected for 16SrRNA sequencing analysis. For DNA
221 extractionOne millilitre of AS S2 sample was extracted in duplicate using the
222 FastDNA® SPIN kit for soil (MP Biomedicals, Solon, USA) according to the
223 manufacturer's instructions. Final DNA products were eluted in a final volume of 50 µL.
224 Afterwards, OneStep™ PCR Inhibitor Removal Kit (Zymo Research, CA, USA) was
225 used in order to remove sample inhibitors which could affect downstream enzymatic
226 reactions such as PCR. Duplicated samples were mixed at 1:1 ratio and DNA measured
227 using Qubit® dsDNA BR Assay Kit (Molecular probes, Eugene, OR, USA). DNA
228 260/280 ratio was measured using the NanoDrop ND-1000 UV/Vis spectrophotometer
229 (NanoDrop Technologies, DE, USA). The hypervariable V3–V4 regionsof bacterial 16S

rRNA gene was amplified in all samples using Illumina primers and following Illumina protocols. Libraries were sequenced on a MiSeq Illumina platform using a 2×300pb paired-end run at Lifesequencing service (Valencia, Spain). Raw DNA sequencing data was processed using QIIME™ 1.9.1 (Caporaso et al., 2010) applying additional scripts available in MicrobiomeHelper virtual box (Comeau et al., 2017). Forward and reverse reads were joined. Joined reads were ckecked for chimeras using Usearch61 algorithm against 16S SILVA_123 database (Quast et al., 2013). Remaining sequences were clustered at 97% similarity into Operational Taxonomic Units (OTUs) using the denovoOTU clustering script. The most abundant sequence of each OTU was picked as its representative, which was used for taxonomic assignment against 16S SILVA_128 database at 97% identity (cut-off level of 3%) using default parameters.

2.7. Statistical analysis

ANOVA simple analysis was carried out using the software STATGRAPHICS Centurion XVII to study the relation between the COD removal efficiencies, BSI (%) and Phylum classification in terms of *Proteobacteria* and *Bacteroidetes* (dependent variables) and the mixed liquor conductivity values (independent variable). Mixed liquor conductivity was studied for different levels: 1, 2, 3, 4 corresponding each level with conductivities until 10 $mS \cdot cm^{-1}$, from 10 to 20 $mS \cdot cm^{-1}$, from 20 to 30 $mS \cdot cm^{-1}$ and from 30 to 40 $mS \cdot cm^{-1}$, respectively.

3. Results

3.1. Mixed liquor conductivity and membrane water flux

Fig. 1 shows the mixed liquor conductivity changes during the OMBR operation. The numbers expressing percentages in the figure mean the percentage of tannery wastewater in the OMBR feed. As expected, there was salt accumulation in the bioreactor due both to the reverse salt flux during forward osmosis process and the high rejection capacity of the FO membrane (>97%) (Praveen and Loh, 2016). It can be observed that the mixed liquor conductivity increases progressively from 1.3 $mS \cdot cm^{-1}$ to a final value of 29.8 $mS \cdot cm^{-1}$. It is important to remark that the percentage of tannery waste water in the feed solution had an important influence over the mixed liquor conductivity. The reason was the high salinity of the tannery waste water. The increasing salinity in bioreactor led to a lower osmotic pressure gradient across the FO membrane causing a reduction in the membrane water flux. In this way, the membrane water flux varied between 3.44 LMH and 0.72 LMH during the total OMBR operation time. After each membrane cleaning step, an increase in the membrane water flux was observed. Membrane fouling also had influence on the membrane water flux decrease. In this way, (Luo et al., 2017) also reported that both phenomena contribute to the membrane water flux decline in the FO process.

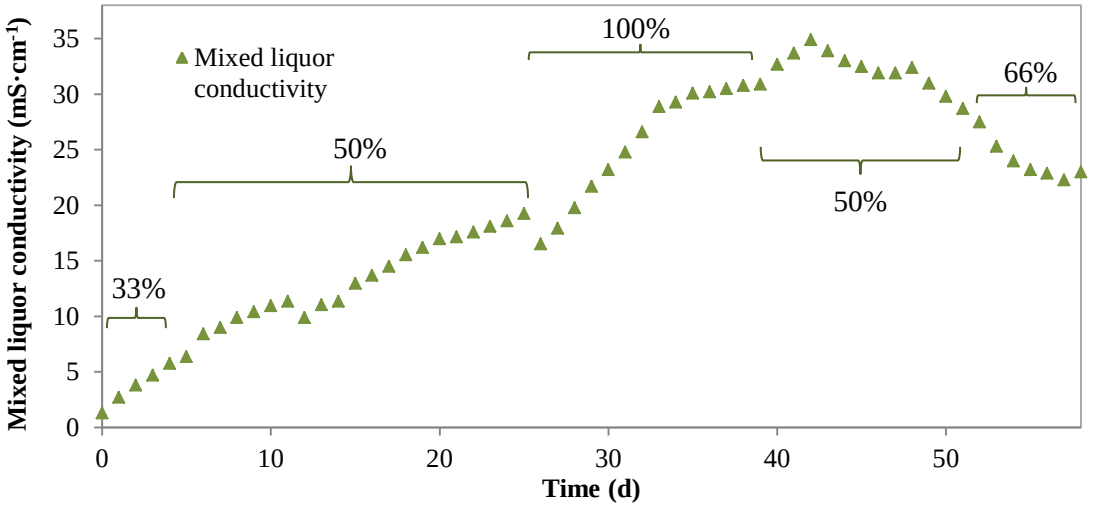

Figure 1: Mixed liquor conductivity evolution during the OMBR operation.

3.2. OMBR efficiency

OMBR organic matter removal efficiency can be calculated as the difference between COD in the feed wastewater and the permeate COD divided by the feed wastewater COD. In this way, the COD considered is that of the stream passing through the membrane to the draw solution side. As the organic matter in the permeate stream was negligible due to the high FO membrane rejection, efficiency results were almost 100%. However, it does not mean that the biological COD removal efficiency was high. In fact, it does not provide any information about the biological process.

COD removal efficiency may also be calculated considering the soluble COD in the OMBR which could give a more accurate parameter to find out the biological degradation occurring in the OMBR. Nevertheless, the accumulation of non-biodegradable COD could also provide confusing values. This is the reason why the study of the bacterial activity and the bacterial stress index among other biological parameters proposed in this work is very helpful to assess the biological process. In this

way, the final values included in Table 2 (COD removal efficiency percentage) could indicate either biological process deterioration or an excessive accumulation of non-biodegradable COD from the tannery wastewater. The decrease of the COD removal efficiency in the reactor could also be associated to negative effects of salinity build-up on biomass activity. Anyway, despite the slight gradual decrease, the overall COD removal efficiencies were maintained near 80% during the first 50 days of operation at increasing conductivity values. However, it seems that around 35 $mS \cdot cm^{-1}$ the conductivity began to affect the overall COD removal efficiency (%). High salinity damages the microbial metabolism and, as a consequence, the biological treatment (Wang et al., 2017a).

Table 2: COD removal efficiencies during the OMBR operation.

Period (d)	COD removal efficiency (%)
0-10	85.65 ± 5.0
11-20	76.06 ± 5.0
21-30	80.38 ± 5.0
31-40	75.67 ± 5.0
41-50	75.85 ± 5.0
51-60	64.53 ± 5.0

3.3. Biological mixed liquor characterization

3.3.1. DNA

DNA concentration in the soluble fraction of the mixed liquor has been represented in Fig. 2 in order to analyse eventual cell lysis. It is observed that DNA concentrations increased as mixed liquor conductivity rose. As salinity decreased in the OMBR due to

313 the mixing of tannery and synthetic wastewater, DNA concentrations in the biomass
314 also decreased gradually. It means that DNA concentration was directly related to the
315 conductivity in the reactor. Zuriaga-Agustí et al., 2012 reported that a slight diminution
316 in the COD removal efficiency was connected to the increment of DNA concentration
317 in the reactor as a consequence of cell disintegration.
318

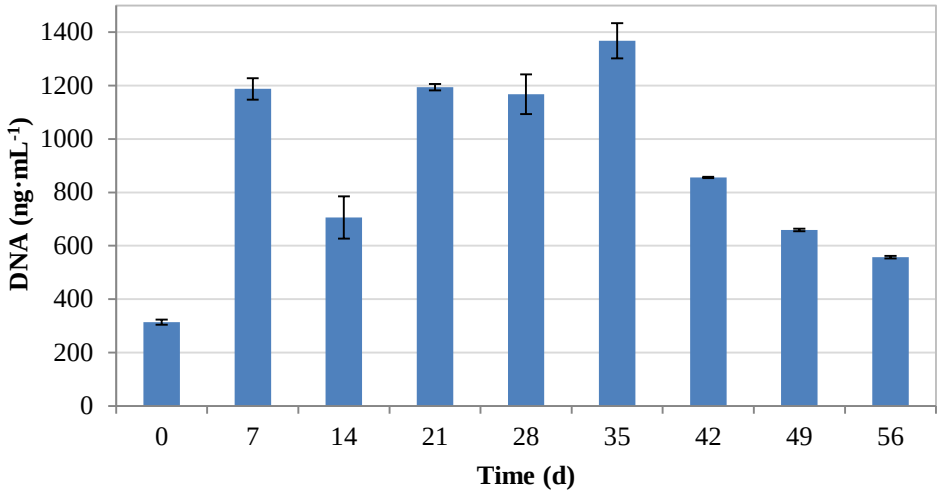

319
320 **Figure 2: DNA concentrations in the soluble fraction of the mixed liquor.**
321
322
323
324 3.3.2. MHEA
325 Fig. 3 shows the α-D-glucosidase and β-D-glucuronidase (Fig. 3.a), alkaline
326 phosphatase, acid phosphatase and dehydrogenase (Fig. 3.b), lipase (Fig. 3.c) and
327 protease (Fig. 3.d) MHEA.
328

From Fig. 3.a, two features can be remarked. On the one hand, glucuronidase activities values remained almost constant during the total experimental period. On the other hand, the glucosidase activity increased until 27th day, but from this day on it remained almost constant. It indicates that the salinity build-up did not affect these enzymes. By contrast, acid phosphatase, alkaline phosphatase and dehydrogenase did not show a clear trend, though started to decrease from the 42nd operation day. As explained above (Section 3.3.1), cell lysis decreased from the 42nd operation day, which can be connected with the reduction of these activities. Ferrer-Polonio et al., 2017 also noted a simultaneous decrease in the DNA concentrations and activity values. It has to be commented that the peak of alkaline phosphatase on the 13th operation day might be due to a deficit of phosphorous concentration in the influent wastewater. Cortés-Lorenzo et al., 2012 showed that enzymatic activities (glucosidase, alkaline phosphatase, acid phosphatase, protease and esterase) were reduced when the salinity was increased in the influent of a submerged fixed bed film reactor. The minimum in the dehydrogenase activity is also to be highlighted, since this value was measured coinciding with the highest conductivity value in the mixed liquor. In other words, the process deterioration by an excessive salinity was indicated by the minimal value of the dehydrogenase activity. Chen et al., 2018 also found that salinity inhibited the dehydrogenase activity of activated sludge.

It can also be observed in Fig. 3.c and Fig. 3.d that lipase and protease activities were maintained practically constant in the six first samples (until the day 36th operation day). Then, they began increasing. It occurred when DNA concentration in the soluble fraction of the OMBR was very high due to the accumulation of cellular debris caused by cell lysis. These substances are mainly proteins and lipids, which are consumed by

354 certain bacterial classes in the named cryptic growth. The same phenomenon of increase
355 of the protease activity associated to the cryptic growth was reported by (Yan et al.,
356 2008) in tests of sludge reduction by thermal treatment.
357
358 Cell lysis releases these compounds, including saccharides, into the medium becoming
359 part of the organic matter biodegradable by the biomass (Uma-Rami et al., 2012). Thus,
360 the protease and lipase enzymatic activities enhanced the hydrolysis of proteins and
361 lipids (Fig 3.a and Fig. 3.d). In other words, cell lysis led to an increase of these
362 enzymes (Li et al., 2009) in spite of an overall reduction of active volatile suspended
363 solids (AVSS), which were reduced down to 500 $mg \cdot L^{-1}$ according to the calculations
364 carried out from the ATP data (section 3.3.3).
365
366 a)
367

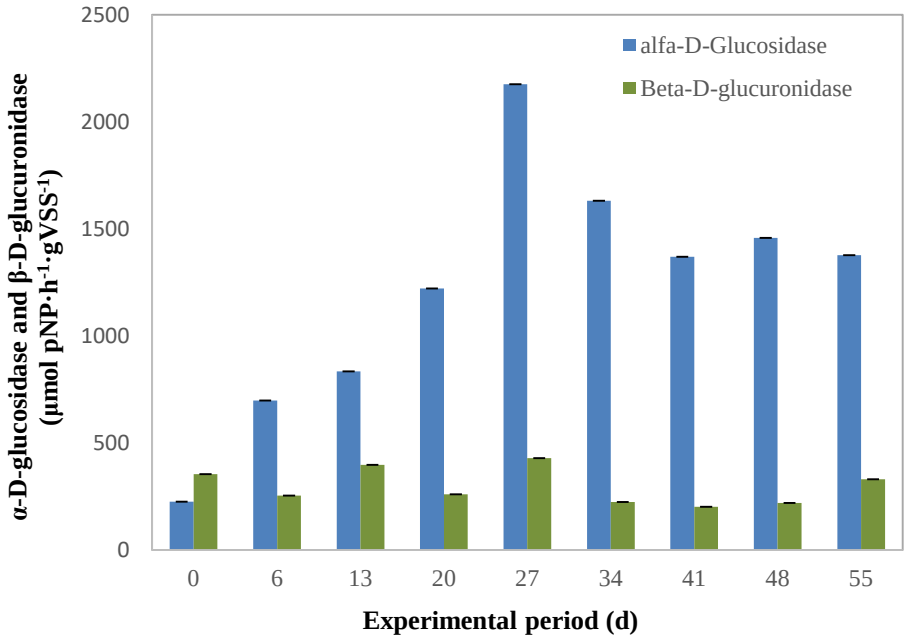

368
369
370

371 b)

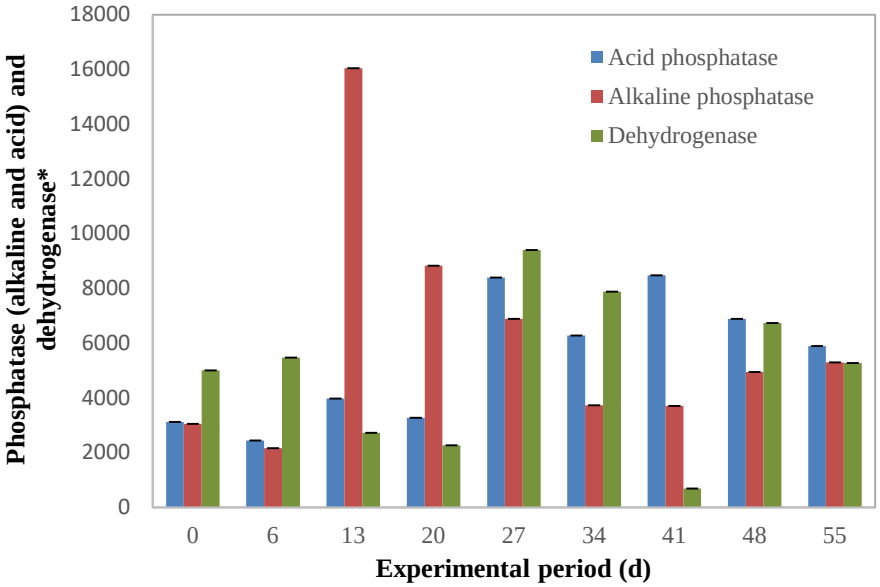

372

373

374 c)

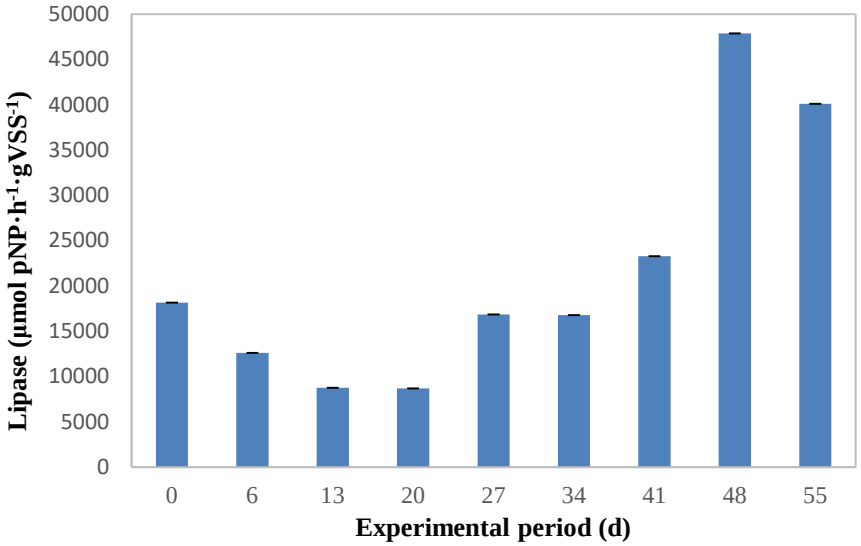

375

376 d)

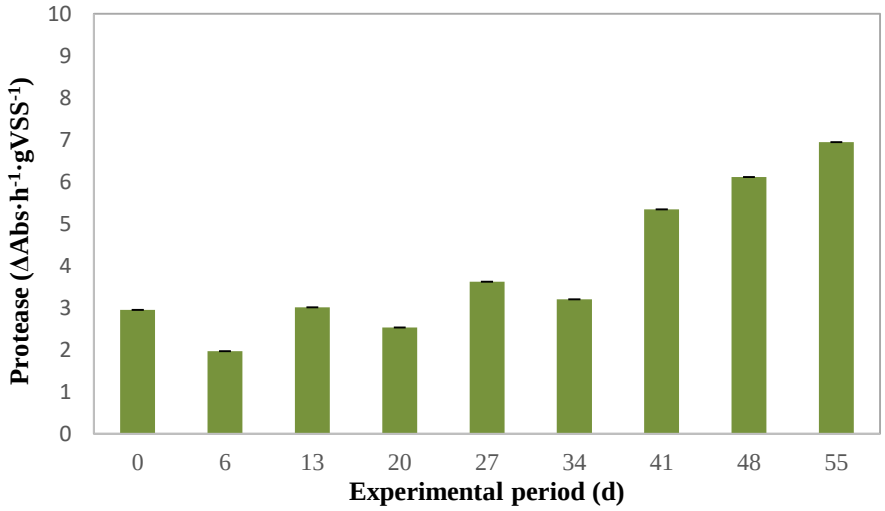

Figure 3: MHEA activities a) α-D-glucosidase and β-D-glucuronidase, b) alkaline phosphatase, acid phosphatase and dehydrogenase, c) lipase and d) protease.
***The units of acid phosphatase and alcaline phosphatase are µmol pNP·h^{-1}·$gVSS^{-1}$ and the units of D-dehidrogenase are µmol formazan·h^{-1}·$gVSS^{-1}$.**

3.3.3. ATP

Bacterial metabolism includes energy generation (catabolism) and energy consumption for anabolism. During both metabolic processes, free energy is conserved in form of ATP after several electron transfer and biochemical reactions. On the one hand, the ability of bacteria to synthesize ATP is very important since this parameter represents the total energy molecule necessary for life. In addition, decreasing the production of ATP will cause the lack of energy for an optimal microbial growth, motility and nutrients transport (Feng et al., 2014).

Fig. 4 plots tATP and dATP concentrations during the entire OMBR operation time. tATP and dATP were normalized with respect to the VSS. In addition, Fig. 4 also shows the BSI index calculated from tATP and dATP. As it can be observed, BSI index increased until the 13th day of operation. Since then, that parameter decreased until the day 41st of operation, probably due to the biomass acclimation to the OMBR saline conditions. From this point on, BSI index was unstable and began increasing indicating the gradual deterioration of the biological process as well as insignificantly low anabolism activity. These results were in concordance with DNA concentrations showed in Fig. 2 since BSI and DNA followed the same trend. In the last sample (55th day) tATP value was practically the same as in the two earlier measurements, though BSI decreased, indicating a recovery in the biological process due to the salinity decrease and the mixing of the tannery effluent with simulated wastewater.

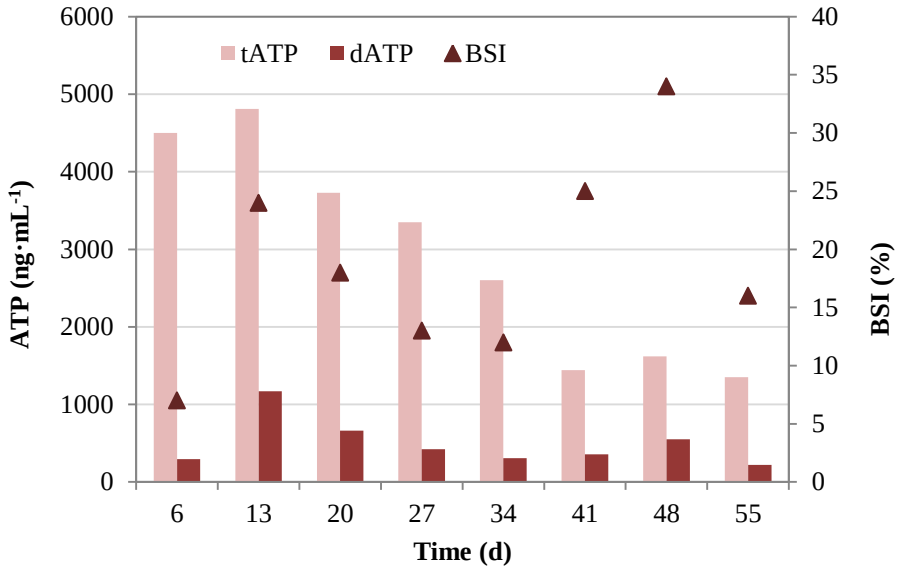

Figure 4: ATP concentrations and BSI index evolution in the mixed liquor.

3.3.4. Relative abundance of bacterial phylotypes

Microbiota rarefaction curves showing microbiota diversity in OMBR samples are showed in Fig. 5. Each curve shows the average number of OTUs found in a given number of sampled sequences. Rarefaction curves were all calculated at the 97% similarity. In total, 417,126 raw reads were obtained from all five OMBR samples. After filtering, 330,474 high-quality sequences were produced. The number of reads of all samples was normalized to the sample with the lowest number of reads (33,238). Fig. 5, demonstrated that the bacterial phylotype richness of the sample 1S (day 5^{th}) was much higher than the other samples.

Salinity build-up in the biological reactor could affect the evolution of microbial community. Overall microbiota compositions for each sample at the phylum and class levels are shown in Fig. 6. In total, 37 phyla were identified in the biomass but only the phyla with relative abundance higher than 1% are shown in Fig. 6.a. Bacterial sequences

affiliated with *Proteobacteria* were the most abundant (relative abundance varying between 50.29% and 34.78%), specifically the first 34 days of operation. After that, sequences affiliated with *Bacteroidetes* were detected in a greater extent varying the relative abundance of this phylum between 27.20% and 40.45%. These results were in concordance with other authors (Wang et al., 2014; Zhang et al., 2016; Zhao et al., 2014) who worked with aerobic activated sludge and have demonstrated that the dominant phyla presented in activated sludge were *Proteobacteria* and *Bacteroidetes.* In addition, Liang et al., 2016 confirmed that *Proteobacteria* and *Bacteroidetes* are the main bacteria in the microbial composition in the activated sludge treating tannery wastewater. Chen et al., 2018 found that *Bacteroidetes* survive easier under the salt stress. The phyla *Planctomycetes* and *Firmicutes* also increased from 1.67% (S1) and 0.96% (S1) to 4.27% (S5, day 55^{th}) and 3.96%, respectively. Inversely, Chen et al., 2018 observed a decreasing trend of *Planctomycetes* when the salinity reached 20 $g \cdot L^{-1}$. *Firmicutes* could survive even when salinity in SBR increased to 20 $g \cdot L^{-1}$. The anaerobic fermentative bacteria of the order *Halanaerobiales* (*Firmicutes*) consist of halophiles (Oren, 2008). When the salinity increased, *Halanaerobiales* increased from 0.055 (S1) to 1.42% (S5). *Halanaerobiales* accumulate salt rather than organic solutes to balance their cytoplasm with their medium (Oren, 2008). (Wang et al., 2017) reported that *Planctomycetes* was less sentitive to salinity than other phyla.

Fig. 6.b. represents the different subclasses of *Proteobacteria* phylum. As it can be observed in Fig. 6.b, the dominant subclasses of *Proteobacteria* are *Alphaproteobacteria*, *Betaproteobacteria* and *Gammaproteobacteria*. During the OMBR operation, the relative abundance of *Alphaproteobacteria* and *Gammaproteobacteria* increased from 26.77% to 58.53 and from 13.90% to 15.31%, respectively. By contrast, the relative abundances of *Betaproteobacteria* decreased from 45.07% to 22.89%. These results were in concordance

455 with (Liang et al., 2016) who also treated tannery wastewater biologically and published
456 that mostly *Alpha-, Beta- and Gamma-proteobacteria* predominated in all samples.
457
458 Regarding *Bacteroidetes* subclasses, Fig. 6.c. shows that the main bacteria presents are
459 *Sphingobacteria* and *Flavobacteria*. *Sphingobacteria* was the predominant class during
460 the first 34 days of operation time, but its abundance was seriously affected by salinity
461 build-up. The decrease of *Sphingobacteria* is influenced by salinity (Chen et al., 2018).
462 However, *Flavobacteria* and Cytophaga were not affected by the high salinity content
463 since its abundance even increased during the last days of the experiment. These results
464 are in agreement with (Cortés-Lorenzo et al., 2014) who also noted the same tendency
465 studying the biological treatment of saline urban wastewater. *Flavobacteria* and
466 *Cytophaga* are the most abundant group detected in the marine systems (Kirchman
467 2002).

468 Sequences of the most abundant OTUs (>0.1%) (Supplementary Table S1) were
469 classified at genus level against Silva128 database. Relative abundances of major genera
470 detected among five samples are shown in Supplementary material Table S1. The genera
471 *Candidatus* Microthrix, *Methylophilus*, *Flavobacterium*, *Ferruginibacter*, *Thauera*,
472 *Zooglea*, *Terrimonas*, *Methyloversatilis*, *Nitrospira*, *Sphaerotilus* and *Acidovorax* were
473 dominant (>1%) in sample S1. By contrast, the dominant genera (>1%) in sample S5
474 were: *Leadbetterella*, *Filomicrobium*, *Algoriphagus*, *Sphingopyxis*, *Gelidibacter*,
475 *Cellulophaga*, *Hyphomicrobium*, *Planctomyces*, *Marivirga*, *Rhodococcus*, *Pseudomonas*
476 y *Arenibacter*. Members of these genera commonly exist in marine environments
477 (Johansen et al., 1999; Kim et al., 2008; Lin et al., 2015; Martineau et al., 2013;
478 Nedashkovskaya et al., 2004; Santina et al., 2015; Zhang et al., 2015). Halotolerant
479 genera are presented in Table S2. During the OMBR operation, the relative abundance of

480 *Leadbetterella* increased from 0.13% to 6.49%. (Ding et al., 2016) also identified
481 *Leadbeterrella* in bulk sludge of OMBR treating anaerobic bioreactor effluent. Growth of
482 *Leadbetterella* strains occurs in the presence of 1% ClNa but not 3% (Weon et al., 2005).
483
484 The EPS producing-bacteria play a significant role in membrane fouling. When impacted
485 by salinity, sludge microorganisms secret EPS (He et al., 2017). (Yeon et al., 2009)
486 revealed that quorum sensing is strongly related to biofilm formation in membrane
487 bioreactors. The quorum sensing (QS) related bacteria during the experimental period
488 were classified following the QS list of (Jo et al., 2016). The relative abundances of QS
489 genera are shown in Table S3. We found differences in relative abundances of QS
490 bacteria. The QS *Flavobacterium* (7.19% vs 0.76%) and *Rhodobacter* (1.79% vs 0.20%)
491 decreased in comparison with *Pseudomonas* (0.18% vs 1.29%) and *Arcobacter* (0.06% vs
492 0.77%).
493
494 The excess growth of filamentous bacteria had significant influence on membrane fouling
495 (Meng et al., 2006).The filamentous bacterial genera identified during the OMBR
496 operation are listed in order of abundance in Table S4. *Candidatus* Microthrix was
497 dominant in sample S1 (5.70%) whereas *Rhodococcus* was dominant in sample S5
498 (1.35%). Foaming filamentous bacteria from mycolata group (*Rhodocccus*,
499 *Mycobacterium* and *Gordonia*) were detected at different abundances. The most abundant
500 foaming bacteria was *Rhodococcus*. The most abundant bulking bacteria was *Candidatus*
501 Microthrix 5.70% (S1) followed by *Sphaerotilus* 1.44% (S1). The *Nostocoida* filament
502 morphotypes I (*Trichococcus*), II (*Candidatus* Alysiosphaera and *Tetrasphaera*) and III
503 (*Isosphaera*) were also identified.

The relative abundances of the nitrifying bacteria responsible for ammonia (*Nitrosomonas*) and nitrite oxidation (*Nitrospira*) are shown in Table S5. The salinity affected NOB but not AOB during the OMBR operation. The abundance of *Nitrosomonas* was 0.31% (day 6) and 0.32% (day 55). The abundance of *Nitrospira* was reduced from 1.45% (day 5^{th}) to 0% (day 55^{th}). (Wang et al., 2017) found that *Nitrospira* could survive at 5 g NaCl, but is inhibited over 10 g NaCl. Bacteria capable of denitrification belong to a variety of groups and include a wide range of physiological traits (Sousa and Bhosle, 2011). Among the denitrifying bacteria, sequences were identified as *Mesorhizobium*, *Rhodobacter*, *Thauera*, *Hyphomicrobium*, *Pseudomonas*, *Paracoccus*, *Castellaniella*, *Halomonas*, *Hyphomonas*, *Zooglea*, *Rhizobium*, *Acidovorax*, *Alcaligenes Azoarcus* and *Comamonas* (Table S5). The dominant (>1% at day 55) halotolerant potential denitrifiers genera were *Mesorhizobium*, *Thauera*, *Hyphomicrobium* and *Pseudomonas*.

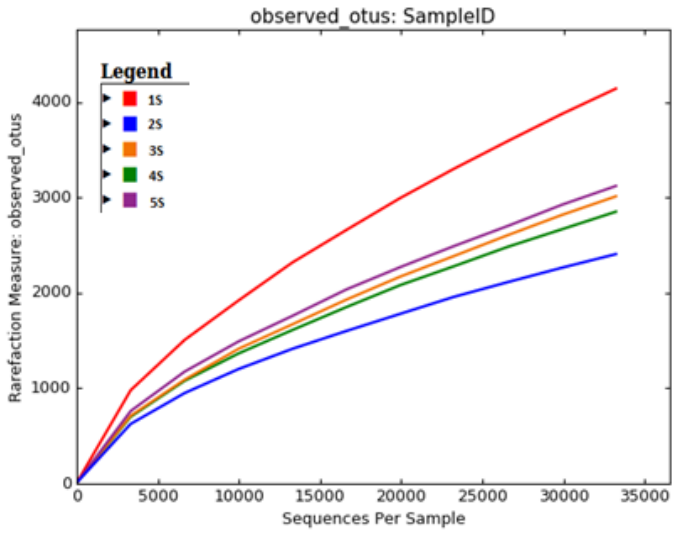

Figure 5: Rarefaction curves of each sample.

521 a)

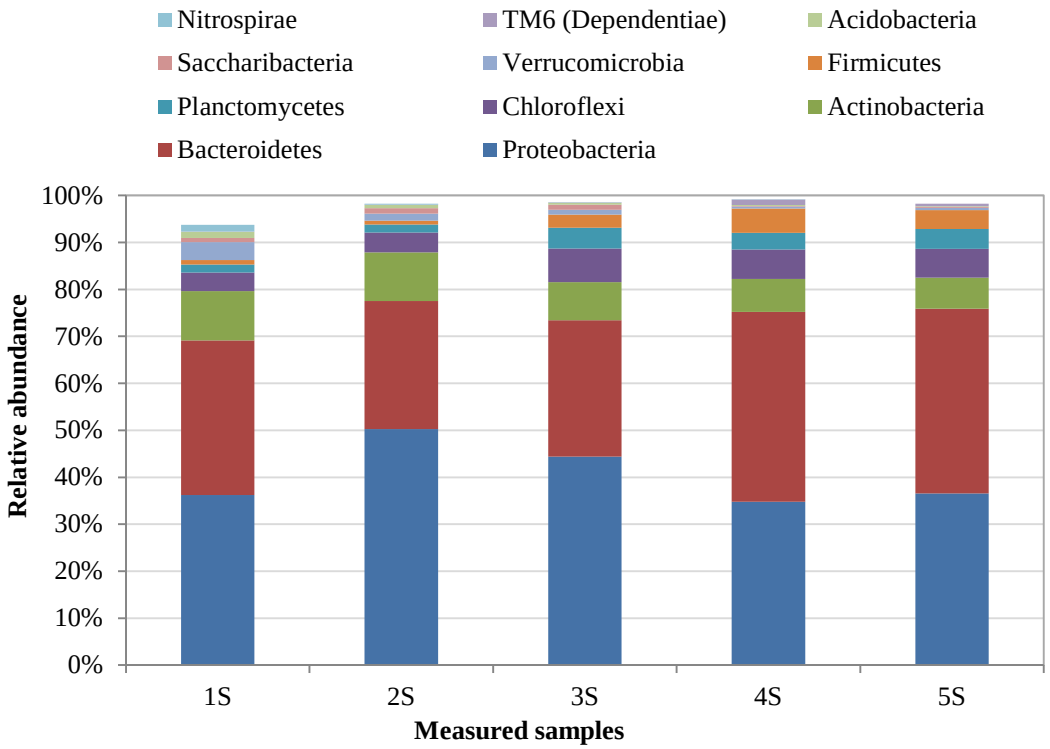

522

523 b)

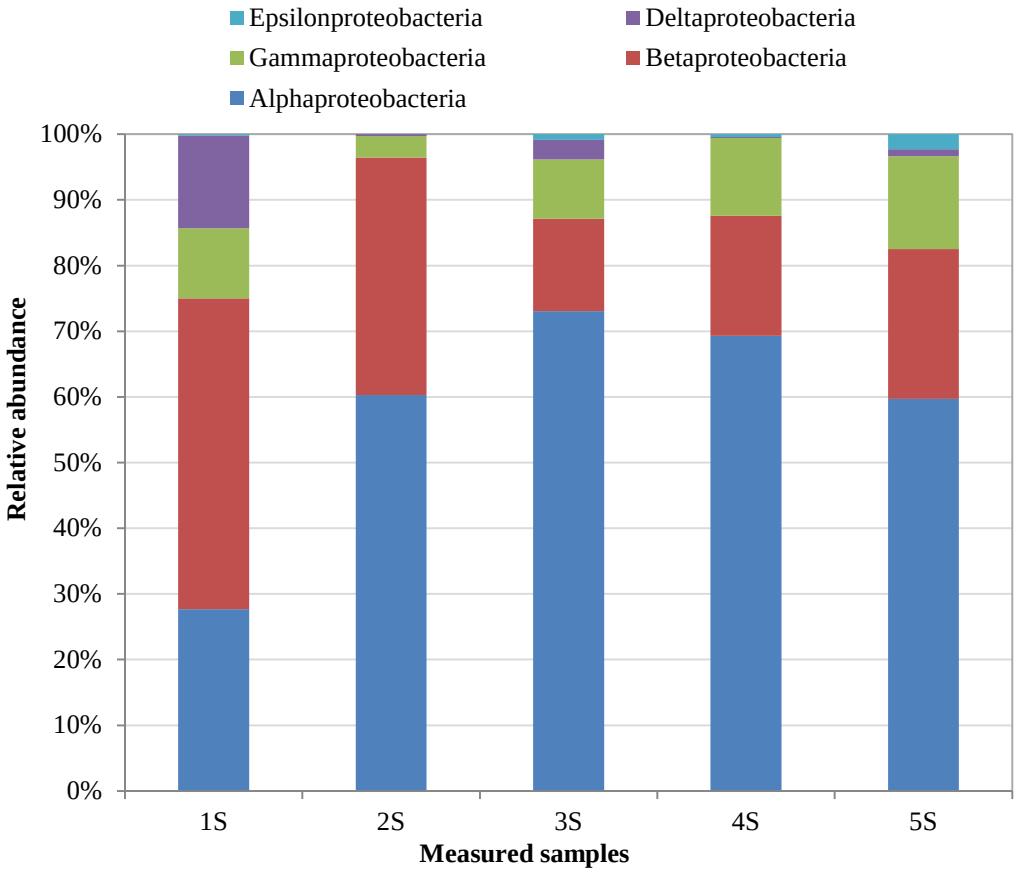

524

c)

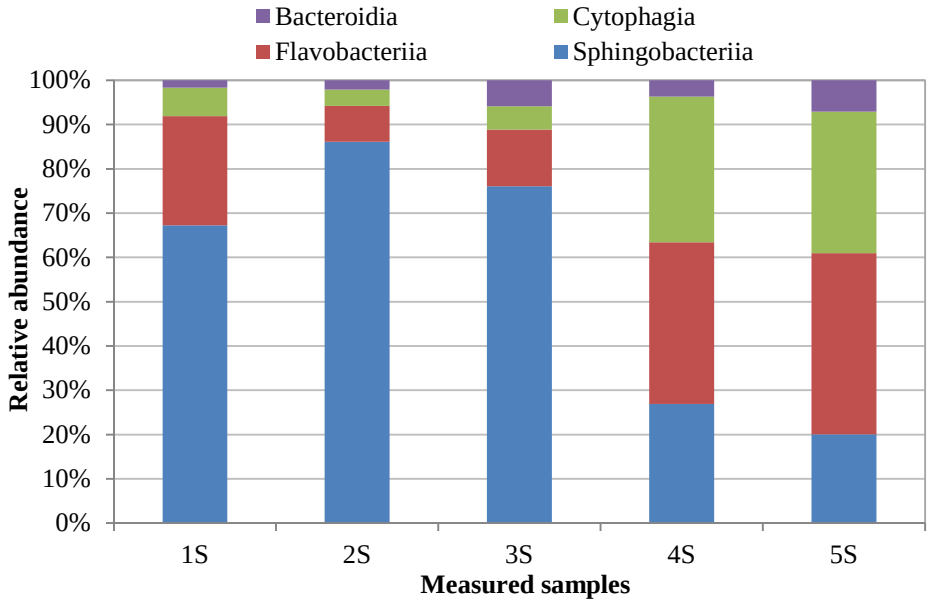

Figure 6: Changes in the microbial community structure a) at the phylum level during the OMBR operation, b) relative abundance of classes of *Proteobacteria* and c) relative abundance of subclasses of *Bacteroidetes*.

3.4. Statistical study

One-way ANOVA was analyzed to study the relation between the COD removal efficiencies, BSI (%) and Phylum classification in terms of *Proteobacteria* and *Bacteroidetes* (dependent variables) and the mixed liquor conductivity values (independent variable). In this way, Table 3 shows the p-value and the F-ratio for each variable studied. It can be concluded that there were statistically significant differences for COD removal efficiencies since p-value was lower than 0.05 (p-value was 0.0018) and F-ratio differs significantly of 1 (F-ratio was 6.55) indicating that the null hypothesis of equality of means of the COD removal efficiencies was rejected.

Although p-value for BSI was slightly higher than 0.05, its low value and the F-ratio indicated an influence of the conductivity on the BSI.

Tukey diagram was plotted in Fig. 7 to evaluate the statistical significant differences between the different levels of conductivities. As it can be observed in Fig. 7, there were only statistical significant differences between the level 1 and 2. Thus, when mixed liquor conductivities were higher than 20 $mS \cdot cm^{-1}$ the COD removal efficiencies began to decrease, which was associated to a process deterioration. This was corroborated by the higher BSI values.

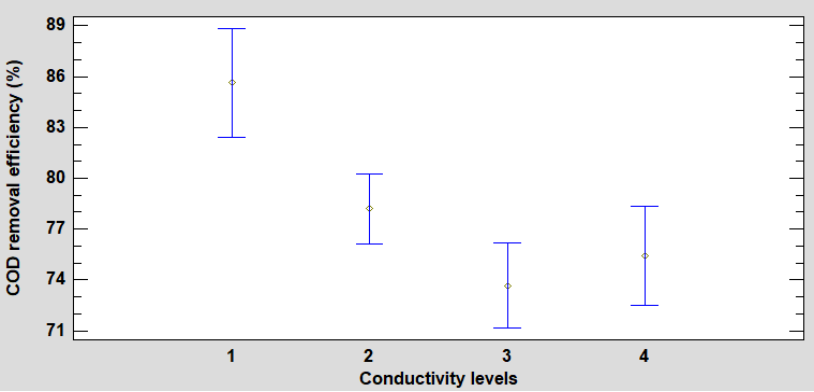

Figure 7: Tukey diagram for COD removal efficiency.

Table 3: p-value and F-ratio for each variable studied.

Variable	p-value	F
COD removal, r (%)	0.0018	6.55
BSI (%)	0.0755	5.07
Phylum (% Bacteroidetes)	0.6963	0.65
Phylum (% Proteobacteria)	0.5868	1.06

Conclusions

In this work, the performance of an OMBR treating tannery wastewater has been evaluated. In this type of reactors salinity and non-biodegradable COD are accumulated due to the high rejection of the FO membranes. In addition to it, the reverse salt flux contributes to a faster conductivity increase in the reactor.

Process monitoring is difficult because COD removal efficiencies data avoid finding out the actual performance of the biological process. Thus, a series of biological indicators have been studied. Results indicated that process deterioration occurs when conductivity reached 35 $mS \cdot cm^{-1}$. The deficient process performance was associated with an increase of the lipase and protease activities, which indicated an increase of lipids and proteins associated to the cell lysis as soluble DNA analysis confirmed. The maximal conductivity entailed a dramatic decrease of the dehydrogenase activity, whose value rose again after the mixing of the tannery effluent with simulated wastewater in order to diminish the reactor conductivity.

The process can also be monitored from ATP analyses. The bacterial stress index as the quotient between dissolved ATP and total ATP was an appropriate indicator to calculate the active biomass and consequently the process performance.

Concerning the microbial population, *Proteobacteria* were the bacterial sequences more abundant followed by *Bacteroidetes.* However, the relative abundance of Bacteroidetes increased when reactor salinity increased.

As general conclusion it can be stated that the treatment of tannery wastewaters by OMBR is limited by salinity accumulation in the reactor. According to the results, after 40 operation days the influent and the non-biodegradable conductivity have to be diminished and sludge has to be withdrawn in order to restore the bacterial activity.

586 More studies at larger scale would be necessary to find out whether the process is
587 sustainable and economically feasible.

588

589 **References**

590

591 Caporaso, J.G., Kuczynski. J., Stombaugh, J., Bittinger, K., 2010. QIIME allows
592 analysis of high-throughput community sequencing data. Nat. Methods,
593 correspondende, 7, 335–336.
594 Chen, Y., He, H., Liu, H., Li, H., Zeng, G., Xia, X., Yang, C., 2018. Effect of salinity
595 on removal performance and activated sludge characteristics in sequencing batch
596 reactors. Bioresour. Technol. 249, 890–899. doi:10.1016/j.biortech.2017.10.092
597 Comeau, A.M., Douglas, G.M., Langille, M.G.I., 2017. Microbiome Helper: a Custom
598 and Streamlined Workflow for Microbiome Research. mSystems, book of chapter.
599 Cortés-Lorenzo, C., Rodríguez-Díaz, M., López-Lopez, C., Sánchez-Peinado, M.,
600 Rodelas, B., González-López, J., 2012. Effect of salinity on enzymatic activities in a
601 submerged fixed bed biofilm reactor for municipal sewage treatment. Bioresour.
602 Technol. 121, 312–319.
603 Cortés-Lorenzo, C., Sipkema, D., Rodríguez-Díaz, M., Fuentes, S., Juárez-Jiménez, B.,
604 Rodelas, B., Smidt, H., González-López, J., 2014. Microbial community dynamics in a
605 submerged fixed bed bioreactor during biological treatment of saline urban wastewater.
606 Ecol. Eng. 71, 126–132.
607 Ding, Y., Tian, Y., Liu, J., Li, N., Zhang, J., Zuo, W., Li, Z., 2016. Investigation of
608 microbial structure and composition involved in membrane fouling in the forward
609 osmosis membrane bioreactor treating anaerobic bioreactor effluent. Chem. Eng. J. 286,

198–207.

Drioli, E., Cortese, B., 1980. Ultrafiltration processes for pollution control and chemical reuse in the tanning industry. Desalination 34, 131–139.

Fababuj-Roger, M., Mendoza-Roca, J.A., Galiana-Aleixandre, M.V., Bes-Piá, A., Cuartas-Uribe, B., Iborra-Clar, I., 2007. Reuse of tannery wastewaters by combination of ultrafiltration and reverse osmosis after a conventional physical-chemical treatment. Desalination 204, 219–226.

Feng, X.C., Guo, W.Q., Yang, S.S., Zheng, H.S., Du, J.S., Wu, Q.L., Ren, N.Q., 2014. Possible causes of excess sludge reduction adding metabolic uncoupler, 3,3',4',5-tetrachlorosalicylanilide (TCS), in sequence batch reactors. Bioresour. Technol. 173, 96–103.

Ferrer-Polonio, E., Fernández-Navarro, J., Alonso-Molina, J.L., Amorós-Muñoz, I., Bes-Piá, A., Mendoza-Roca, J.A., 2017. Changes in the process performance, sludge production and microbial activity in an activated sludge reactor with addition of a metabolic uncoupler under different operating conditions. J. Environ. Manage. 203, 349–357.

George, J.S., Ramos, A., Shipley, H.J., 2015. Tanning facility wastewater treatment : Analysis of physical – chemical and reverse osmosis methods. J. Environ. Chem. Eng. 3, 969–976.

Gu, J., Cai, H., Yu, S.L., Ri, Q., Yin, B, Guo, Y.F., Zhao, J.Y., Wu, X.L., 2007. Marinobacter gudaonensis sp. nov., isolated from an oil-polluted saline soil in a Chinese oilfield. Int J. Syst. Evol. Microbiol. 57, 250–254.

Gu, Y., Chen, L., Ng, J.W., Lee, C., Chang, V.W.C., Tang, C.Y., 2015. Development of anaerobic osmotic membrane bioreactor for low-strength wastewater treatment at mesophilic condition. J. Memb. Sci. 490, 197–208.

He, H., Chen, Y., Li, X., Cheng, Y., Yang, C., Zeng, G., 2017. Influence of salinity on microorganisms in activated sludge processes: A review. Int. Biodeterior. Biodegrad. 119, 520–527.

Hickenbottom, K.L., Hancock, N.T., Hutchings, N.R., Appleton, E.W., Beaudry, E.G., Xu, P., Cath, T.Y., 2013. Forward osmosis treatment of drilling mud and fracturing wastewater from oil and gas operations. Desalination 312, 60–66.

Hoover, L.A., Phillip, W.A., Tiraferri, A., Yip, N.Y., Elimelech, M., 2011. Forward with Osmosis: Emerging Applications for Greater Sustainability. Environ. Sci. Technol. 45, 9824–9830.

Jo, S.J., Kwon, H., Jeong, S.Y., Lee, C.H., Kim, T.G., 2016. Comparison of microbial communities of activated sludge and membrane biofilm in 10 full-scale membrane bioreactors. Water Res. 101, 214–225.

Johansen, J.E., Nielsen, P., Sjraholm, C., 1999. Description of Cellulophaga baltica gen. nov., sp. nov. and Cellulophaga fucicola gen. nov., sp. nov. and reclassification of [Cytophaga] lytica to Cellulophaga lytica gen. nov., comb. nov. Int. J. Syst. Bacteriol. 49, 1231–1240.

Kandasamy, K., Tharmalingam, K., Velusamy, S., 2017. Treatment of tannery effluent using sono catalytic reactor. J. Water Process Eng. 15, 72–77.

Kim, B.S., Lim, Y.W., Chun, J., 2008. Sphingopyxis marina sp. nov. and Sphingopyxis litoris sp. nov., isolated from seawater. Int J Syst Evol Microbiol. 58, 2415–2419.

Kirchman, D.L., 2002. The ecology of Cytophaga–Flavobacteria in aquatic environments. The ecology of Cytophaga–Flavobacteria in aquatic environments. FEMS Microbiol. Ecol. 39, 91–100.

Le-clech, P., Chen, V., Fane, T.A.G., 2006. Fouling in membrane bioreactors used in wastewater treatment. J. Memb. Sci. 284, 17–53.

660 Li, X., Ma, H., Wang, Q., Matsumoto, S., Maeda, T., Ogawa, H.I., 2009. Isolation,
661 identification of sludge-lysing strain and its utilization in thermophilic aerobic digestion
662 for waste activated sludge. Bioresour. Technol. 100, 2475–2481.
663 Liang, H., Ye, D., Li, P., Su, T., Wu, J., Luo, L., 2016. Evolution of bacterial consortia
664 in an integrated tannery wastewater treatment process. RSC Adv. 6, 87380–87388.
665 Lin, C.Y., Zhang, X.Y., Liu, A., Liu, C., Song, X.Y., Su. H.N., Qin, Q.L., Xie, B.B.,
666 Zhang,Y.Z., 2015. Marivirga atlantica sp. nov., isolated from seawater and emended
667 description of the genus Marivirga. Int. J. Syst. Evol. Microbiol. 65, 1515–1519.
668 Luján-Facundo, M.J., Soler-Cabezas, J.L., Mendoza-Roca, J.A., Vincent-Vela, M.C.,
669 Bes-Piá, A., 2017. A study of the osmotic membrane bioreactor process using a sodium
670 chloride solution and an industrial effluent as draw solutions. Chem. Eng. J. 322, 603–
671 610.
672 Luo, W., Hai, F.I., Price, W.E., Elimelech, M., Nghiem, L.D., 2016. Evaluating ionic
673 organic draw solutes in osmotic membrane bioreactors for water reuse. J. Memb. Sci.
674 514, 636–645.
675 Luo, W., Phan, H. V, Xie, M., Hai, F.I., Price, W.E., Elimelech, M., Nghiem, L.D.,
676 2017. Osmotic versus conventional membrane bioreactors integrated with reverse
677 osmosis for water reuse: Biological stability, membrane fouling, and contaminant
678 removal. Water Res. 109, 122–134.
679 Maharaja, P., Mahesh, M., Chitra, C., Kalaivani, D., Srividya, R., Swarnalatha, S.,
680 Sekaran, G., 2017. Sequential oxic-anoxic bio reactor for the treatment of tannery saline
681 wastewater using halophilic and filamentous bacteria. J. Water Process Eng. 18, 47–57.
682 Martineau, C, Villeneuve, C, Mauffrey, F, Villemur, R., 2013. Hyphomicrobium
683 nitrativorans sp. nov., isolated from the biofilm of a methanol-fed denitrification system
684 treating seawater at the Montreal Biodome. Int. J. Syst. Evol. Microbiol. 63, 3777–

685 3781.
686 Mendoza-Roca, J.A., Galiana-Aleixandre, M.V., Lora-García, J., Bes-Piá, A., 2010.
687 Purification of tannery effluents by ultrafiltration in view of permeate reuse. Sep. Purif.
688 Technol. 70, 296–301.
689 Meng, F., Zhang, H., Yang, F., Li, Y., Xiao, J., Zhang, X., 2006. Effect of filamentous
690 bacteria on membrane fouling in submerged membrane bioreactor. J. Memb. Sci. 272,
691 161–168.
692 Mosca, D., Stazi, V., Daugulis, A.J., Tomei, M.C., 2017. Treatment of synthetic tannery
693 wastewater in a continuous two-phase partitioning bioreactor : Biodegradation of the
694 organic fraction and chromium separation. J. Clean. Prod. 152, 321–329.
695 Nedashkovskaya, O.I., Vancanneyt, M., Van Trappen, S, Vandemeulebroecke, K.,
696 Lysenko, A.M., Rohde, M., Falsen, E., Frolova, G.M., Mikhailov, V.V., 2004.
697 Description of Algoriphagus aquimarinus sp. nov., Algoriphagus chordae sp. nov. and
698 Algoriphagus winogradskyi sp. nov., from sea water and algae, transfer of Hongiella
699 halophila Yi and Chun 2004 to the genus Algoriphagus as Algoriphagus halophilus
700 comb. n. Int. J. Syst. Evol. Microbiol. 1757–1764.
701 Nguyen, L.H., Chong, N., 2015. Development of an ATP measurement method suitable
702 for xenobiotic treatment activated sludge biomass. J. Chromatogr. B 1000, 69–76.
703 Oren, A., 2008. Microbial life at high salt concentrations: phylogenetic and metabolic
704 diversity. Saline Systems, 4, 1-13.
705 Praveen, P., Loh, K.C., 2016. Osmotic membrane bioreactor for phenol biodegradation
706 under continuous operation. J. Hazard. Mater. 305, 115–122.
707 Qiu, G., Ting, Y.P., 2013. Osmotic membrane bioreactor for wastewater treatment and
708 the effect of salt accumulation on system performance and microbial community
709 dynamics. Bioresour. Technol. 150, 287–297.

710 Quast, C., Pruesse, E., Yilmaz, P., Gerken, J., Schweer, T., Yarza, P., Peplies, J.
711 Glöckner, F.O., 2013. The SILVA ribosomal RNA gene database project: improved
712 data processing and web-based tools. Nucleic Acids Res 41, D590–D596.
713 Santisi, S., Simone, C., Catalfamo, M., Mancini, G., Hassanshahian, M., Lucrezia, G.,
714 Giuliano, L., Yakimov, M.M., 2015. Biodegradation of crude oil by individual bacterial
715 strains and a mixed bacterial consortium. Braz J Microbiol. 46, 377–387.
716 Sousa, T., Bhosle, S., 2011. Microbial Denitrification and Its Ecological Implications in
717 the Marine System. Microorganisms in Environmental Management. Chapter 1683–
718 700.
719 Suganthi, V., Mahalakshmi, M., Balasubramanian, N., 2013. Development of hybrid
720 membrane bioreactor for tannery ef fl uent treatment. Desalination 309, 231–236.
721 Uma Rani, R., Adish Kumar, S., Kaliappan, S., Rajesh Banu, I.T., 2012. Low
722 temperature thermo-chemical pretreatment of dairy waste activated sludge for anaerobic
723 digestion process. Bioresour. Technol. 103, 415–424.
724 Wang, X., Chang, V.W.C., Tang, C.Y., 2016. Osmotic membrane bioreactor (OMBR)
725 technology for wastewater treatment and reclamation: Advances, challenges, and
726 prospects for the future. J. Memb. Sci. 504, 113–132.
727 Wang, X., Wang, C., Tang, C.Y., Hu, T., Li, X., Ren, Y., 2017a. Development of a
728 novel anaerobic membrane bioreactor simultaneously integrating micro fi ltration and
729 forward osmosis membranes for low- strength wastewater treatment. J. Memb. Sci. 527,
730 1–7.
731 Wang, X., Zhao, Y., Li, X., Ren, Y., 2017b. Performance evaluation of a
732 microfiltration-osmotic membrane bioreactor (MF-OMBR) during removing silver
733 nanoparticles from simulated wastewater. Chem. Eng. J. 313, 171–178.
734

735 Wang, X.D., Wang, Y.Y., Song , S.K., Wang, Wu, M., Wang, D.L., 2017. Impact of
736 salinity on the performance and microbial community of anaerobic ammonia oxidation
737 (Anammox) using 16S rRNA High-throughput Sequencing technology. Glob. Nest 19,
738 377–388.
739 Wang, Z, Zhang, X.X., Lu, X, Liu, B., Li, Y., Long, C., Li, A., 2008. Abundance and
740 diversity of bacterial nitrifiers and denitrifiers and their functional genes in tannery
741 wastewater treatment plants revealed by high-throughput sequencing. Bioremediation of
742 Wastewater. Book of chapter, 101–123.
743 Weon, H.Y., Kim, B.Y., Kwon, S.W, Park, I.C., Cha, I.B., Tindall, B.J., Stackebrandt,
744 E. Trüper, Go, S.J., 2005. Leadbetterella byssophila gen. nov., sp. nov., isolated from
745 cotton-waste composts for the cultivation of oyster mushroom. Int. J. Syst. Evol.
746 Microbiol. 55, 2297–2302.
747 Xie, M., Price, W.E., Nghiem, L.D., 2012. Rejection of pharmaceutically active
748 compounds by forward osmosis: Role of solution pH and membrane orientation. Sep.
749 Purif. Technol. 93, 107–114.
750 Yan, S., Miyanaga, K., Xing, X.H., Tanji, Y., 2008. Succession of bacterial community
751 and enzymatic activities of activated sludge by heat-treatment for reduction of excess
752 sludge. Biochem. Eng. J. 39, 598–603.
753 Yang, W., Cicek, N., Ilg, J., 2006. State-of-the-art of membrane bioreactors: Worldwide
754 research and commercial applications in North America. J. Memb. Sci. 270, 201–211.
755 Yeon, K.M., Cheong, W.S., Oh, H.S., Lee, W.N., Hwang, B.K., Lee, C.H., Haluk, B.,
756 Lewandowski, Z., 2009. Quorum Sensing: A New Biofouling Control Paradigm in a
757 Membrane Bioreactor for Advanced Wastewater Treatment. Environ. Sci. Technol. 43,
758 380–385.
759

760 Zhang, Y., Li, B., Xu, R.X., Wang, G.X., Zhou, Y., Xie, B., 2016. Effects of
761 pressurized aeration on organic degradation efficiency and bacterial community
762 structure of activated sludge treating saline wastewater. Bioresour. Technol. 222, 182–
763 189.
764 Zhang, D.C., Margesin, R., 2015. Gelidibacter sediminis sp. nov., isolated from a
765 sediment sample of the Yellow Sea. Int. J. Syst. Evol. Microbiol. 65, 2304–2309.
766 Zhao, D., Huang, R., Zeng, J., Yu, Z., Liu, P., Cheng, S., Wu, Q.L., 2014.
767 Pyrosequencing analysis of bacterial community and assembly in activated sludge
768 samples from different geographic regions in China. Appl. Microbiol. Biotechnol. 98,
769 9119–9128.
770 Zuriaga-Agustí, E., Garrido-Mauri, G., Mendoza-Roca, J.A., Bes-Piá, A., Alonso-
771 Molina, J.L., 2012. Reduction of the sludge production in a sequencing batch reactor by
772 addition of chlorine dioxide: Influence on the process performance. Chem. Eng. J. 209,
773 318–324.
774